

Significant Seasonal Contrast in the Arabian Sea During Deglaciation: Evidence From Oxygen Isotopic Analyses of Individual Planktic Foraminifera

Pothuri Divakar Naidu^{1}, Nobuaki Niitsuma², Kaustubh Thirumalai³, Sushant S. Naik¹,**

1. CSIR - National Institute of Oceanography
Dona Paula 403 004, Goa
India

2. Institute of Geosciences, Shizuoka University,
836 Oya, Shizuoka 422-8529, Japan

3. Department of Earth, Environmental, and Planetary Sciences – Brown University
324 Brook Street, Providence, RI 02912, USA

Abstract

The variation of stable isotopes between individual shells of planktic foraminifera of a given species and size may provide short-term seasonal insight into past sea-surface temperature (SST) and salinity (SSS). In this context, oxygen isotope analyses of individual *Globigerinoides sacculifer* were carried out from the Ocean Drilling Program Site 723A in the western Arabian Sea to unravel seasonal changes over the last 22 kyr. $\delta^{18}\text{O}$ values of single shells of *G. sacculifer* range from of 0.54 to 2.09‰ at various discrete depths in the core which spans the last 22 kyr. Maximum inter-shell $\delta^{18}\text{O}$ variability and relatively higher standard deviation is noticed from 20 to 10 kyr (deglaciation), whereas from 10 kyr onwards (Holocene) inter-shell $\delta^{18}\text{O}$ variability decreases. Based on statistical inferences, we interpret this result as greater seasonal SST and SSS contrasts during the deglaciation compared to the Holocene. These winter-to-summer contrasts during the deglaciation can likely be explained by a net reduction in summer upwelling linked to changes in wind forcing and net evaporation-minus-precipitation that might, along with local causes, be related to deglacial shifts in the intertropical convergence zone (ITCZ). We note that a common winter-dominated SST signal in the Arabian Sea and in Greenland was pervasive during the last glacial period, strengthening evidence of a North Atlantic link with Indian Ocean SST. Thus, the present study has wider implications in understanding whether the forcing mechanism of tropical monsoon climate lies in high latitudes or in the tropics.

****Corresponding Author: P. Divakar Naidu (divakar@nio.org)**

Formatted: Font: Not Bold, Italic, Font color: Auto, Complex Script Font: Times New Roman, Not Bold, Italic

Formatted: Font: Not Bold, Italic, Font color: Auto, Complex Script Font: Times New Roman, Not Bold, Italic

Formatted: Left: 0.75", Right: 0.75", Width: 8.27", Height: 11.69"

Formatted: Font: Not Bold, Italic, Complex Script Font: Times New Roman, Not Bold, Italic

Formatted: Font: Italic, Complex Script Font: Times New Roman, Italic

Formatted: Font: (Default) Times New Roman, Italic, Complex Script Font: Times New Roman, Italic

Formatted: Font: Italic, Font color: Auto, Complex Script Font: Times New Roman, Italic

Formatted: Font: Italic, Complex Script Font: Times New Roman, Italic

Formatted: Centered

Formatted: Font: 13 pt, Complex Script Font: 13 pt

Formatted: Centered

Formatted: Font: Bold, Complex Script Font: Bold

Formatted: Centered

Formatted: Justified, Space After: 6 pt, Line spacing: single

Formatted: Space After: 6 pt, Line spacing: single

1. Introduction

The Arabian Sea experiences high seasonal changes in terms of sea surface temperature (SST), biological productivity, and aeolian and fluvial terrigenous material supply predominantly driven by seasonal reversal of southwest (SW) and northeast (NE) monsoon winds. Extensive work has been carried out in understanding monsoon variability on glacial and interglacial timescales (Prell, 1984; Anderson and Prell, 1993), and on millennial time scales (Sirocko et al., 1996; Naidu and Malmgren, 1996; Schulz et al., 1998). Studies have also investigated past SST (Rostek et al., 1997; Dahl and Oppo, 2006; Saher et al., 2007; Rashid et al., 2007; Anand et al., 2008; Govil and Naidu, 2010), fluctuations of oxygen minimum zone (Reichert et al., 1998) and denitrification (Altabet et al., 1995) in the Arabian Sea. Previously, by using transfer functions and artificial neural network techniques on planktic foraminiferal census data, seasonal SST was reconstructed for February and August by CLIMAP (1981), and winter and summer SST by Naidu and Malmgren (2005). Despite extensive studies focusing on SST and seasonal SST gradients, the sea-surface salinity (SSS) signal and its seasonal contrast are poorly known in the geological past of the Arabian Sea. This might be in part because at the scale of coastal seasonality, the Arabian Sea experiences salinity changes far less than changes experienced in the Bay of Bengal, East China Sea, or South China Sea. Here, we attempt to use a novel approach to reconstruct seasonal SSS gradients by using single shell analyses of planktic foraminiferal species *G. sacculifer* coupled with SST-estimates from transfer functions in order to understand the relationship between the monsoon and seasonality over the last 22 kyr in the Arabian Sea.

2. Strategy

Generally, conventional bulk foraminiferal analyses are conducted on 10-to-several foraminiferal tests, where they are combined into a single sample. In this case, assemblages of individuals from which the shells were picked span a large temporal range and thereby represent an average of environmental information. Short-lived events such as episodic or seasonal changes, which were recorded by several individuals, could be masked by the averaged temperature signal, as a typical planktic foraminifer lives for 2-4 weeks (Spero, 1998). On the other hand, isotopic values of single foraminiferal shells hold the ability to trace seasonal and short-lived events through the past. In this connection, variation of stable isotope ratios between individual shells of planktic

Formatted: Space After: 6 pt, Line spacing: 1.5 lines

Formatted: Space After: 6 pt

foraminifera of a given species and size have been used to depict seasonal oceanographic changes in the Pacific (Killingley et al., 1981; Oba, 1990; Spero and Williams., 1990, Leduc et al. 2010, Khider et al. 2011) Mediterranean (Tang and Stott, 1993) and Indian Ocean (Niitsuma et al. 1991; Ganssen et al., 2011). In this study, we have used single shells of *G. sacculifer* for oxygen and carbon isotopic analysis in order to document seasonal changes at the ODP Site 723A from the western Arabian Sea.

3. Oceanography

Circulation in the Arabian Sea is controlled by the seasonal reversal of the SW and NE monsoon winds. During summer (June through September), strong southwesterly winds blow across the Arabian Sea, and cause Ekman transport and intense upwelling along the Oman and Somalia margins and the southwest coast of India (Wyrki, 1973). The upwelling process brings cold, nutrient-rich waters from a few hundred meters depth into the surface and fuels the biological productivity in the euphotic zone and also cools surface waters. Maximum SST prevails prior to the onset of the southwest monsoon and minimum SST occurs during the SW monsoon. Most strikingly, winter SST (NE monsoon) are slightly warmer than summer SST (SW monsoon) (Fig. 1). The salinity signal also contrasts between the SW and NE monsoons (Fig. 1).

4. Material and Methods

Ocean Drilling Program Site 723A is located in the region of intense upwelling and highest sedimentation rate along the Oman Margin in the Arabian Sea (Prell and Niitsuma, 1989) (Fig. 2). Chronology for the Site 723A is based on 13 AMS ¹⁴C ages (Naidu and Malmgren, 2005) and covers the time span of the last 22 kyr (Table 1). We have chosen *G. sacculifer* for single shell analyses because this species lives throughout the year in the Arabian Sea (Curry et al., 1992) and occupies mixed layer depths (Hemelben et al., 1989). Twenty individual shells of *G. sacculifer* (without sac) from the 500 to 600 μm size fraction were set aside in a stainless-steel thimble. Few drops of methyl alcohol were dropped into the thimble where the individual shells were gently cracked by using a thin needle, and cleaned in a ultrasonic bath by viewing the cleaning process under binocular microscope. The cleaned individual carbonate test was reacted in saturated pyrophosphoric acid at 60°C in a vacuum system on-line to a MAT 250 Isotope Ratio Mass Spectrometer with ultra-small sample gas inlet system. The isotopic composition of the evolved CO₂ gas is reported in δ notation as per mil (‰) deviations from PDB and presented in Table 2. Calibration were performed with the standard carbonate NBS-20, assuming its oxygen and carbon isotopic composition versus PDB to be -4.18‰ and -1.07‰ respectively (Craig, 1957). The analytical precision, estimated from repeated

Formatted: Justified, Space After: 6 pt

Formatted: Space After: 6 pt

analyses of un-roasted NBS-20 carbonate reacted under conditions identical to that of the foraminiferal samples was 0.02‰ for carbon 0.05‰ for oxygen. In order to unravel the inter-shell $\delta^{18}\text{O}$ variability caused by seasonal SST and SSS variations, we have used seasonal SST variations estimated by Naidu and Malmgren (2005) to account for the SST factor, and the remaining $\delta^{18}\text{O}$ changes were considered as driven by seasonal SSS (Table 3). Though inherent uncertainties exist in the calculated inter-shell SSS signal, the remnant SST signal is seasonal and constructively interferes with SSS to produce the overall $\delta^{18}\text{O}$ signal. In this regard, the SSS signal dominates inter-shell $\delta^{18}\text{O}$ variability after removing the overall SST signal.

Due to the large annual cycle in this location, we expected the individual foraminiferal $\delta^{18}\text{O}$ signal to reflect changes in seasonality as opposed to changes in interannual (or longer timescales) variability. To test this hypothesis, we utilized the Individual Foraminiferal Approach Uncertainty Analysis (INFAUNAL) forward model (Thirumalai et al. 2013). First, we retrieved monthly SST and SSS at the site from the HadISST (Rayner et al. 2003) and ORA-S4 (Balmaseda et al. 2012) datasets. Next, we forward modeled the *G. sacculifer* $\delta^{18}\text{O}$ signal and perturbed it with analytical and sampling uncertainty ($n = 20$ forams) inherent in our methods. We found that indeed INFAUNAL indicates that the dominant control on the individual foraminiferal signal at this site is due to changes in seasonal contrast (Fig. 3) Hence, we use this statistical inference to interpret our downcore foraminiferal data.

5. Results and Discussions

The $\delta^{18}\text{O}$ values of *G. sacculifer* show a high range (1 to 2‰) of inter-shell variability and large standard deviation ($\sigma > 0.45$) values between 20 and 10 ka and low variability (<1‰) and relatively lower standard deviation values ($\sigma < 0.22$) between 8 to 0.5 ka (Figs. 4 and 5).

The variability of isotopic ratios between shells of the individual specimens of same species at the same stratigraphic level must be due to following four causes as stated by Killingly et al., 1981: 1. Mixing of individuals from older and younger geological periods by organisms on the sea floor (i.e. bioturbation; e.g. Stott and Tang, 1991); 2. Seasonal and longer-term variations in the temperature and isotopic composition of the sea water within which the shells grew (e.g. Spero, 1998; Thirumalai et al. 2013), this might include the influence of eddies in this region (Piontkorski and Nezlin, 2012), which can contribute to variability, based on the lifespan of individual foraminifera (~2-4 weeks) 3. Variations in depth of calcification (e.g. Oba, 1991); and 4. Variations in metabolic or vital effects (e.g. Ezard et al. 2015). Considering that ODP Site 723A is located in the oxygen minimum zone (OMZ) and receives high sedimentation (35 to 60 cm/ka), the effect of

Formatted: Justified, Space After: 6 pt

Formatted: Space After: 6 pt

bioturbation effect is minimal-to-none (Naidu and Malmgren, 1995). The effect of stable isotope variation in depth of calcification would not affect our results because the size range $>500\ \mu\text{m}$ does not influence the ontogenic effect on the oxygen and carbon isotopic ratios in the Indian Ocean (P. D. Naidu, manuscript in preparation, 2018). Therefore, we believe that the individual shell $\delta^{18}\text{O}$ changes reflect the seasonal isotopic changes of water in which the foraminifera grew and thus inter shell $\delta^{18}\text{O}$ variability is interpreted as changes in seasonal temperature and salinity at the core location. Thus, single shell analysis has advantages in inferring seasonal changes and reconstructing short-lived anomalous conditions in ocean history. These changes ought to appear as distinct modes in the distribution of isotopic values at a given time.

5.1. Seasonal SST and SSS Changes

It appears that inter shell $\delta^{18}\text{O}$ variability was higher during the last glacial period than during the Holocene (Fig. 4), but strikingly, the highest variability seems to occur during the deglaciation. This site is located in the intense upwelling zone of the Arabian Sea where part of the documented $\delta^{18}\text{O}$ changes here should reflect temperature variations modulated by the upwelling through time in the western Arabian Sea. Previously, seasonal SST estimates based on the planktic foraminifera census data using artificial neural network techniques show that maximum temperature contrast occurred between 20 and 14 kyr, which were attributed to the variation of upwelling intensity at this site (Naidu and Malmgren, 2005). In addition to weak upwelling, during the last glacial period, there is an evidence for increased dust delivery (Thomson et al., 1997) and perhaps increased aerosol levels in the atmosphere which might further decreases the winter SST in this region. Thus, weak upwelling during summer, strong NE monsoon winds and more aerosol concentrations during winters caused maximum seasonal SST in the western Arabian Sea during the last glacial period. Similarly, upwelling was intense during the Holocene (Naidu and Malmgren, 1996; Overpeck et al., 1996), which lowers the SST during summer, and winter NE monsoon winds were weak during Holocene (Govil and Naidu, 2010), therefore minimum seasonal SST contrasts observed at this site. As the difference in solar insolation changes between summer and winter season at 30°N was maximum from 12 to 6 kyr (Fig. 6) and, as this does not coincide with the maximum seasonal SST difference at this site, this further reveals that SST changes at this location were governed by seasonal upwelling processes rather than solar insolation.

Nevertheless, seasonal SST changes alone cannot account for the inter-shell $\delta^{18}\text{O}$ variability of *G. sacculifer* at this site. We explore the hypothesis that seasonal salinity variations might contribute to the rest of $\delta^{18}\text{O}$ variability after removing seasonally reconstructed temperatures from

Formatted: Space After: 6 pt

the $\delta^{18}\text{O}$ data. Though our approach is semi-quantitative, we find that seasonal SSS contrasts exhibit maximum variability from 18 to 10 kyr (Table. 3). More evaporation during glacial winters compared with summers might have caused these high seasonal SSS gradients inferred from the inter-shell variability. We suggest that changes of evaporation between summer and winter caused by the seasonal migration of ITCZ in the Indian Ocean might explain our observation. Seasonal migration of ITCZ was minimal during the last glacial period (Denton et al., 2005) and as such a more southerly ITCZ during last glacial period would increase the net evaporation minus precipitation during winter in the Oman Margin, thereby causing high SSS anomalies (Fig. 6). Enhanced evaporation during winter not only cools the surface waters but also increases the upper-layer salinity. During summer however, evaporation was reduced due to weak summer monsoon winds thereby lowering SSS. Thus, the seasonal migration of ITCZ would cause major changes in evaporation-minus-precipitation patterns between summer and winter in the western Arabian Sea. Conversely, seasonal migration of ITCZ during the last glacial maximum (21 ka) was minimal (Mc Gee et al., 2014) and evaporation was more or less the same between summer and winter causing minimum seasonal SSS difference. The mean position of the ITCZ moved to north during the Holocene and this might have reduced winter evaporation-minus-precipitation and increases summer upwelling and rainfall causing minimum seasonal SSS contrasts from 9 to 0 kyr in our dataset.

5.2. Comparison with Previous Work

Ganssen et al. (2011) document oxygen isotopes on individual shells of *Globigerinoides. ruber* and *Globigerina bulloides* in a core offshore Somalia (ODP 905) for the Holocene and the last Glacial period. They find higher variability in single-shell $\delta^{18}\text{O}$ during the Holocene compared to that from the glacial period. Furthermore, they interpret the differences in $\delta^{18}\text{O}$ variability as temperature variability in entirety, and conclude that their $\delta^{18}\text{O}$ ranges likely reflect extreme minimum and maximum temperatures during those particular time periods ($\sim 15^\circ\text{C}$ in the Holocene compared to $\sim 11^\circ\text{C}$ in the LGM as interpreted in Ganssen et al., 2011). This presumably contrasts with our results where we find greater variability during the deglaciation in our *G. sacculifer*-based data as compared to the Holocene. Initially, this appears to be a contradictory inference with the Ganssen et al. (2011) dataset from the Somalian margin, around 1,500 km south of the Oman margin. In modern times, these two sites experience seasonal temperature variability that are not dissimilar (standard deviation of the annual cycle is 1.5°C in Somalian margin compared to 1.8°C in the Oman Margin according to the HadISST dataset) and thus it is presumable that they ought to experience similar climatic variability in past periods as well. However, the seasonal salinity variability in the modern is different between the two sites where it is smaller magnitude in the Oman margin ($1\sigma = 0.08$ PSU)

compared to the Somalian margin ($1\sigma = 0.2$ PSU). Our paired dataset reveals 0.1-1.6 PSU SSS variability in the downcore dataset along with 0.4-2.7°C SST variability (Table 3). We contend that seasonal salinity variability was an important factor in the source of $\delta^{18}\text{O}$ variability of single foraminiferal shells at the Oman margin site. Hence, it is presumable that salinity variability was also important in the Somalian margin site. The Ganssen et al. (2011) study doesn't incorporate seasonal salinity variability into their downcore interpretations and this might be one source of uncertainty that contributes to the discrepancy in results. However, there are other reasons why these datasets may not be directly comparable: 1) the number of individual foraminifera used in our study (~20) might be prone to higher uncertainties and hence has the potential to be biased, although the statistical results from INFAUNAL indicate that regardless of this uncertainty, the signal of the datasets is controlled by seasonality, 2) the differences might be due to differences in habitats and seasonality of the different types of foraminifera used in both of the studies, or 3) there might be local differences in hydrography that affect the Somalian margin differently from the Oman margin. Interestingly, our SST estimates using neural networks approximately equal those reconstructed by Ganssen et al. (2011) using Mg/Ca analysis. Furthermore, both of these regions are affected by cold-core eddies, which might add a random component of variability to both single foraminiferal datasets, thereby conflating interpretation. In either case, we contend that $>2\text{‰}$ $\delta^{18}\text{O}$ changes reconstructed by Ganssen et al. (2011) might not reflect temperature changes alone ($>10^\circ\text{C}$).

5.3. Seasonal SST and SSS Contrast and Intertropical Convergence Zone (ITCZ)

Seasonality is a key diagnostic variable of the climate system and mechanism of climate change (Guilderson et al., 2011). Precession of the equinoxes changes the Earth-Sun distance which determines the amount of solar radiation received by the Earth in any particular season. Consequently, the precession cycle of the Earth's orbit exerts an influence on the strength of monsoon winds and variation in seasonality and ITCZ position in the Indian Ocean (Clemens et al., 2003). During boreal summer, the ITCZ migrates northward across the Indian Ocean and the Indian subcontinent, which brings summer monsoon rainfall. During late boreal fall, the ITCZ retreats southward decreasing rainfall. Comparison of annual, summer and winter SST variations at ODP Site 723A reveals that winter SSTs exhibit greater magnitude of variations than summer SSTs since the last glacial period indicating that the dominant influence of winter SSTs in pushing the ITCZ southward. This is consistent with speleothem calcite $\delta^{18}\text{O}$ from Qunf Cave (Fleitmann et al., 2003), proximal to Site 723 A, which indicates that changes in overhead precipitation related to the ITCZ was forced by changes in precession.

Formatted: Justified, Space After: 6 pt

Formatted: Space After: 6 pt

5.4. Greenland and monsoon teleconnection through seasonality:

Monsoon reconstructions based on proxies such as *Globigerina bulloides* abundances (Gupta et al., 2003), total organic carbon record (Schulz et al., 1998) from marine sediment cores from the Arabian Sea and oxygen isotopic ratios of speleotherms from Oman (Fleitmann et al., 2003) and China (Wang et al., 2001) have demonstrated that abrupt changes in monsoon intensity coincide with temperature changes indicated in the north Atlantic Ocean and/or in Greenland GISP2 ice core record. In the same way, millennial-scale paleoclimate records of the last glaciation show striking similarities across a huge area of the planet from Greenland to eastern Asia (Denton et al., 2005). These similarities include not only the number and spacing, but also the relative magnitudes of stades and interstades in monsoon records, for example $\delta^{15}\text{N}$ (Altabet et al., 2003) and productivity records (Singh et al., 2011) from the Arabian Sea. Such similarities, in millennial scale climate records between Greenland and in the tropics imply that a common forcing mechanism transmits the paleoclimate signal from Greenland to Asia.

Previously, it has been speculated by Denton et al (2005) that winter-dominated seasonality switches of North Atlantic and Greenland might be driving the millennial-scale oscillations of the Atlantic ITCZ (Hughen et al., 1996), the Asian monsoon (Schulz et al., 1999; Wang et al., 2001) and surface and intermediate waters of eastern North Pacific (Hendy and Kennett, 1999). But it is not known whether winter-dominated temperature in Greenland influence the tropical winter temperature, in this context our data of individual shell $\delta^{18}\text{O}$ of *G. sacculifer* lends support that the winter temperature in the Arabian Sea also show strong seasonality during deglaciation (Fig. 6). Therefore, it is proposed here that winter seasonality was the common forcing linkage between Greenland-European temperatures, the Atlantic ITCZ and Asian monsoons. The consequences of changes in seasonality in Greenland propagated millennial scale abrupt climate change in the northern hemisphere and into the tropics (Denton et al., 2005). Further, a tenfold increase of dust during stadials in Greenland (Mayewski et al., 1997) which is derived from the deserts of western China (Biscaye et al., 1997) provides an additional atmospheric link not only to the summer monsoon but also to the winter monsoons.

In Greenland the switches in mean annual temperature were dominated by large winter changes, and thus temperatures during winter control the seasonality in Greenland (Denton et al., 2005). Existence of identical Greenland and monsoon signals at millennial scale particularly between 10 and 60 ka (Schulz et al., 1998; Wang et al., 2001) and maximum seasonal SST difference during last glaciation as evident from the present study would reveal that winter dominated seasonality was common in both the regions. Severe Greenland winters would reduce the winter temperature over

Formatted: Space After: 6 pt

Eurasia leading to heavy snow fall in the western Himalayas result in weakening or collapse of Indian summer monsoon (Blanford, 1884) and thus large Eurasian snowpack would cause large scale regional climate change. Recent studies have also emphasized the relationship between spatial pattern of snow cover in Tibet and summer monsoon (Zhao and Moore, 2004). Late-lasting winter snowfall carries over well into the summer, thus slowing summer warming of the Asian land mass and reducing the land-sea temperature contrast that is a primary driver of the summer monsoon. Modeling studies also confirm that a link between the Eurasian snow cover during winters to follow on summer monsoons (Barnett et al., 1988), which offers a physical mechanism whereby long-lasting winter snow cover on the Eurasian land mass during glacial stades would link a weak Asian summer monsoon with cold Greenland and European winter temperatures.

Abrupt millennial scale fluctuations were not present during Holocene in the Greenland temperature records but Indian and Asian monsoon records document greater magnitude fluctuations during Holocene (Wang et al., 2001; Gupta et al., 2003; Fleitman et al., 2003; Govil and Naidu, 2010). This reveals that minimum seasonal shifts between winter and summer temperatures in the Greenland would be unable to propagate the temperature signal to the monsoon influenced regions causing asynchrony between Greenland and Asian Monsoon records during the Holocene. Thus, Holocene variability in the Indian and Asian monsoon records is perhaps forced by the solar insolation changes rather than the Greenland temperatures.

6. Conclusions

Individual shells of planktic foraminiferal species *G. sacculifer* were analyzed for oxygen isotopes at ODP Site 723A, which provides insights into SST and SSS seasonality over the last 22 kyr in the western Arabian Sea. Inter-shell $\delta^{18}\text{O}$ values of *G. sacculifer* exhibit higher standard deviation during the deglaciation compared with the Holocene, and are driven by maximum seasonal SST and SSS changes in the western Arabian Sea.

This increase in deglacial SSS seasonality can be explained by the increase of winter evaporation and reduction of monsoonal rainfall, contrasting with the Holocene where increased rainfall and reduced evaporation result in minimal SSS seasonality. This result is bolstered by seasonal SST inferences where maximal SST seasonality during the deglaciation occurs due to greater winter cooling and reduced summer upwelling. Both evaporation and precipitation processes are coupled with the seasonal migration of ITCZ in the western Arabian Sea, wherein its movement can potentially explain the variability in our inter-shell data.

Acknowledgements

We thank Japan Society for the Promotion of Higher Studies (JSPS) for providing financial support. KT thanks the Brown University Presidential Postdoctoral Fellowship for support. This is National Institute of Oceanography Contribution.....

References

- Altabet, M.A., Francois, D., Murray, W., Prell, W.L., 1995. Climate-related variations in denitrification in the Arabian Sea from 15N/14N ratios. *Nature* 373, 506-509.
- Anand, P., Kroon, D., Singh, A.D., Ganeshram, R.S., Ganssen, G., Elderfield, H., 2008. Coupled sea surface temperature–seawater $\delta^{18}\text{O}$ reconstructions in the Arabian Sea at the millennial scale for the last 35 ka. *Paleoceanography* 23, PA4207, doi:10.1029/2007PA001564.
- Anderson, D.M., Prell, W.L., 1993. A 300 kyr record of upwelling off Oman during the late Quaternary: evidence of the Asian southwest monsoon. *Paleoceanography* 8, 193–208.
- Barnett, T., Dumenil, L., Schlese, U., Roeckner, E., 1988. The effect of Eurasian snow cover on global climate. *Science* 239, 504-507.
- Balmaseda, M. A., Mogenssen, K., Weaver, A. T., 2012. Evaluation of the ECMWF ocean reanalysis system ORAS4. *Quat. J. Roy. Meteorol. Soc.* **139**, 1132–1161.
- Biscaye, E., Grousset, F.E., Revel, M., Van der Gaast, S., Zielinski, G.A., Vaars, A., Kukla, G., 1997. Asian provenance of glacial dust (stage 2) in the Greenland Ice Sheet Project 2 Ice Core, Summit, Greenland. *J. Geophys. Res.*, 102, 26,765-26,781.
- Blanford, H.F., 1884. On the connection of the Himalayan snowfall with dry winds and seasons of drought in India. *Proceedings of the Royal Society of London* 37, 3-22.
- Clemens, S.C., Prell, W.L., 2003. A 350,000 year summer monsoon multi-proxy stack from the Owen Ridge, Northern Arabian Sea. *Mar. Geol.*, 201, 35-51.
- CLIMAP Project Members 1981. Seasonal Reconstruction of the Earth' Surface at the Last Glacial Maximum, Map MC 36, Geol.Soc.Am., Boulder, Colorado.
- Craig, H., 1957. Isotopic standards for carbon and oxygen and correction factors for mass-spectrometric analysis of carbon dioxide. *Geochimica et Cosmochimica Acta* 12, 133–149.
- Curry, W.B., Ostermann, D.R., Guptha, M.V.S., Ittekkot, V., 1992. Foraminiferal production and monsoonal upwelling in the Arabian Sea: Evidence from sediment traps, in *Upwelling Systems: Evolution Since the Early Miocene*, edited by C.P. Summerhayes, W.L. Prell, and K.C. Emeis, Geol. Soc. Spec. Publ. London, 64, 93-106.
- Dahl, A.K., Oppo, D.W., 2006. Sea surface temperature pattern reconstructions in the Arabian Sea. *Paleoceanography* 21, PA1014, doi: 10.1029/2005PA001162.

- Denton, G.H., Alley, R.B., Comer, G.C., Broecker, W.S., 2005. The role of seasonality in abrupt climate change. *Quat. Sci. Rev.*, 24, 1159-1182.
- Ezard, T.H., Edgar, K.M., Pincelli, M.H., 2015. Environmental and biological controls on size-specific $\delta^{13}\text{C}$ and $\delta^{18}\text{O}$ in recent planktonic foraminifera. *Paleoceanography*, 30, 151-173, doi:10.1002/2014PA002735.
- Fleitmann, D., Burns, S.J., Mudelsee, M.U., Neff, J., Kramers, Mangini, A and Matter, A., 2003. Holocene forcing of the Indian monsoon recorded in a stalagmite from Southern Oman. *Science* 300, 1737-1739.
- Ganssen, G.M., Peeters, F.J.C., Metcalfe, B., Anand, P., Jung, S.J.A., Kroon, D., Brummer, G.J.A., 2011. Quantifying sea surface temperature ranges of the Arabian Sea for the past 20000 years. *Climate of the Past*. 7, 1337-1349.
- Govil, P., Naidu, P.D. 2010. Evaporation-precipitation changes in the eastern Arabian Sea for the last 68ka: Implications on monsoon variability. *Paleoceanography*, 25, PA1210, doi:10.1029/2008PA001687.
- Guilderson, T.P., Fairbanks, R.G., Rubenstone, J.L., 2001. Tropical Atlantic coral oxygen isotopes: glacial-interglacial sea surface temperature and climate change. *Mar. Geol.*, 172, 75-89.
- Gupta, A.K., Anderson, D.M., Overpeck, J.T., 2003. Abrupt changes in the Asian southwest monsoon during the Holocene and their links to the North Atlantic Ocean. *Nature* 421, 354-356.
- Haug, G.H., Hughen, K.A., Sigman, D.M., Peterson, L.C., Rohl, U., 2001. Southward Migration of the Intertropical Convergence Zone through the Holocene. *Science*, 293, 1304-1306.
- Hemleben, Ch., Spindler, M., Anderson, O.R., 1989. *Modern Planktonic Foraminifera*, Springer Verlag, Berlin, 363pp.
- Hendy, I., Kennet, J., 1999. Latest Quaternary North Pacific surface water responses imply atmosphere-driven climate instability, *Geology*, 27, 291-294.
- Hughen, K.A., Overpeck, J.T., Peterson, L.C., Trumbore, S., 1996. Rapid climate changes in the tropical Atlantic region during the last deglaciation. *Nature*, 380, 51-54.
- Khider, D., Stott, L.D, Emile-Geay, J., Thunell, R., Hammond, D.e., 2011. Assessing El Nino Southern Oscillation variability during the past millennium, *Paleoceanography*, 26, PA3222, doi:10.1029/2011PA002139.

- Killingley, J.S., Johnson, R.F., Berger, W.H., 1981. Oxygen and carbon isotopes of Individual shells of planktonic foraminifera from Ontong-Java Plateau, Equatorial Pacific. *Palaeogeogr. Palaeoclimatol. Paleocol.*, 33, 193-204.
- Leduc, G., Vidal, L., Catrapanis, O., and Bard, E., 2009. Mode of eastern equatorial Pacific thermocline variability: Implications for ENSO dynamics over the last glacial period. *Paleoceanography*, 24, PA3202, doi:10.1029/2008PA001701.
- Lee, K.E., Park., Y.G., 2003. Seasonal changes in sea surface temperature of the subtropical north Pacific during the last glaciation. *Geosci. J.*, 7, 129-133.
- Levitus, S., Burgett, R., Boyer, T.P., 1994. World Ocean Atlas 1994, Salinity, NOAA Atlas NESDIS 3, U. S. Department of Commerce, Washington, DC, 99pp.
- Mayewski, A., Meeker, L.D., Twickler, M.S., Whitlow, S., Yang, Q., Lyons, W.B., Prentice, M., 1997. Major features and forcing of high-latitude northern hemisphere atmospheric circulation using a 110,000-year long glaciochemical series. *J. Geophys. Res.*, 102, 26345-26366.
- McGee, D., Donohoe, A., Marshewll, J., Ferreira, D., 2014. Changes in ITCZ location and cross equatorial heat transport at the Last Glacial Maximum, Heinrich Stadial 1, and the mid-Holocene. *Earth and Planetary Science Letters*, 390, 698-79.
- Naidu, P.D., Malmgren, B.A., 1996. A high-resolution record of late Quaternary upwelling along the Oman Margin, Arabian Sea based on planktonic foraminifera. *Paleoceanography* 11, 129–140.
- Naidu, P.D., Malmgren, B.A., 2005. Seasonal Sea Surface Temperature Contrast Between the Holocene and Last Glacial Period in the Western Arabian Sea (ODP Site 723A): Modulated by Monsoon Upwelling. *Paleoceanography* 20, PA1004, doi:10.1029/2004PA001078.
- Niituma, N., Oba, T., Okada, M., 1991. Oxygen and carbon isotope stratigraphy at Site 723, Oman Margin, *Proceedings of Ocean Drilling Program Scientific Results*, 117, 321-341.
- Oba, T., 1990. Paleoceanographic Information Obtained by the Isotopic Measurement of Individual Foraminiferal Specimens, *Proceedings of the First International Conference on Asian Marine Geology*, Shanghai, 169-180.
- Overpeck, J.T., Anderson, D.M., Trumbore, S., Prell, W.L., 1996. The southwest Indian monsoon over the last 18,000 years. *Clim. Dyn.*, 12, 213–225.
- Piontkorski, S.A., Nezhlin, N.P., 2012. Mesoscale Eddies of Arabian Sea: Physical-biological Interactions. *Int. J. of Marine Sciences*, 2, 51-56.

- Prell, W.L., 1984. Variation of monsoonal upwelling: a response to changing solar radiation, in *Climatic Processes and Climate sensitivity*, edited by J. E. Hansen and T. Takahashi, A. G. U., Maurice Ewing Ser., 5, 48-57.
- Prell, W.L., Niitsuma, N., 1989. Site 723, Proceedings of Ocean Drilling Program Initial Reports 117, 319-384.
- Rashid, H., Flower, B.P., Poore, R.Z., Quinn, T.M., 2007. A ~25 ka Indian Ocean monsoon variability record from the Andaman Sea. *Quat. Sci. Rev.*, 26, 2586-2597.
- Rayner, N. A. *et al.* 2003. Global analyses of sea surface temperature, sea ice, and night marine air temperature since the late nineteenth century. *J. Geophys. Res.* **108**, 4407–37.
- Reichart, G.J., Lourens, L.J., Zachariasse, W.J., 1998. Temporal variability in the northern Arabian Sea Oxygen Minimum Zone (OMZ) during the last 225, 000 years. *Paleoceanography* 13, 607-621.
- Rostek, F., Ruhland, G., Bassinot, F.C., Muller, P.J., Labeyrie, L.D., Lancelot, Y., Bard, E., 1993. Reconstructing sea surface temperature and salinity using $\delta^{18}\text{O}$ and alkenone records. *Nature*, 364, 319-321.
- Saher, M.H., Jung, S.J.A., Elderfield, H., Greaves, M.J., Kroon, D., 2007. Sea surface temperatures of the western Arabian Sea during the last deglaciation. *Paleoceanography* 22, PA2208, doi:10.1029/2006PA001292.
- Schulz, H.S., Von Rod, U., Erlenkeuser, H., 1998. Correlation between Arabian Sea and Greenland climate oscillations of the past 110,000 years. *Nature* 393, 54-57.
- Singh, A.D., Jung, S.J.A., Darling, K., Ganeshram, R., Ivanochko, T., Kroon, D., 2011. Productivity collapses in the Arabian Sea during glacial cold phases. *Paleoceanography*, 26, PA3210, doi:10.1029/2009PA001923.
- Sirocko, F., Garbe-Schonberg, D., McIntyre, A., Molfino, B., 1996. Teleconnection between the subtropical monsoons and high latitude climates during the last deglaciation. *Science* 272, 526-529.
- Spero, H.J., 1998. Life history and stable isotope geochemistry of planktonic foraminifera, In *Isotope Paleobiology and Paleoecology*, edited by R.D. Norris and R.M. Corfield, pp. 7-36, Paleontol. Soc. Pap., Pittsburg, Penn.
- Spero, H.J., Williams, D.F., 1990. Evidence for seasonal low-salinity surface waters in the Gulf of Mexico over the last 16,000 years. *Paleoceanography* 5, 963-975.

- Tang, C.M., Stott, L.D., 1993. Seasonal salinity changes during Mediterranean sapropel deposition 9000 years BP: Evidence from isotopic analyses of individual planktonic foraminifera. *Paleoceanography* 8, 473-493.
- Thirumalai, K., Partin, J. W., Jackson, C. S. & Quinn, T. M. Statistical constraints on El Niño Southern Oscillation reconstructions using individual foraminifera: A sensitivity analysis. *Paleoceanography* 28, 401–412 (2013).
- Thompson, L.G., Davis, H.E., Henderson, K.A., Mosley-thompson, E., Lin, P.N., Beer, J., Synal, H.A., Cole-Doi, J., Bolzan, H.F., 1997. Tropical climate instability: the last glacial cycle from a Qinhai Tibetan Ice Core. *Science* 276, 1821-1825.
- Wang, Y.J., Cheng, H., Edwards, R.L., An, Z.S., Wu, J.Y., Shen, C.C., Dorale, J.A., 2001. A high-resolution absolute-dated late Pleistocene monsoon record from Hulu Cave, China. *Science* 294, 2345-2348.
- Wyrki, K., 1973. Physical oceanography of the Indian Ocean, Vol. 3 of Ecological studies: analysis and synthesis, in *Biology of the Indian Ocean*, edited by B. Zeischel and S. A. Gerlach, pp. 18-36, London: Chapman and Hall Ltd.
- Zhao, H., Moore, G.W.K., 2004. On the relationship between Tibetan snow cover, the Tibetan plateau monsoon and the Indian summer monsoon. *Geophys. Res. Lett.*, 31, L14204.

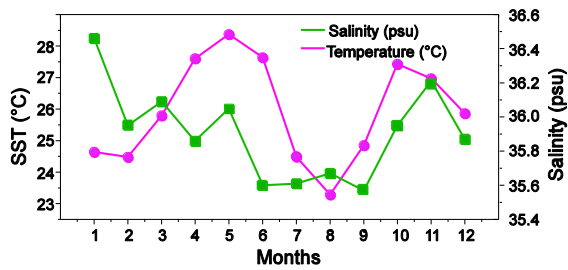


Figure 1. Variations of Sea surface temperature and salinity at the location of ODP Site 723A in the western Arabian Sea (Levitus et al., 1994). Lowest sea surface temperature values during July, August and September caused by SW monsoon upwelling. More evaporation during winter months results in high sea surface salinity during NE monsoon.

Formatted: Font: Bold, Complex Script Font: Bold

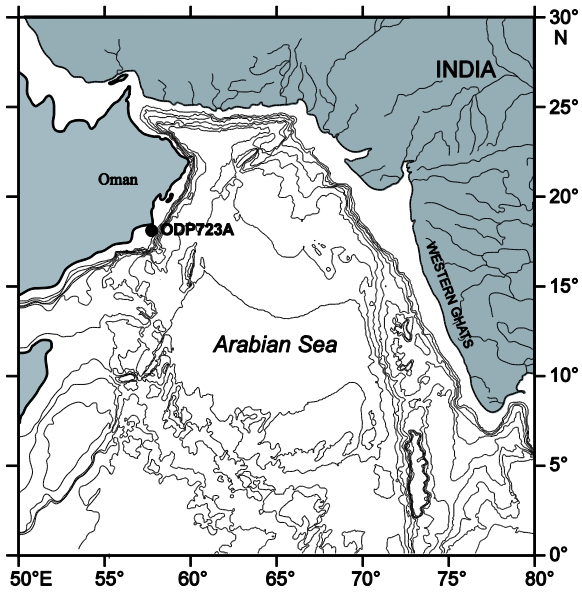


Figure 2. Location of ODP Site 723A in the western Arabian Sea.

Formatted: Font: Bold, Complex Script Font: Bold

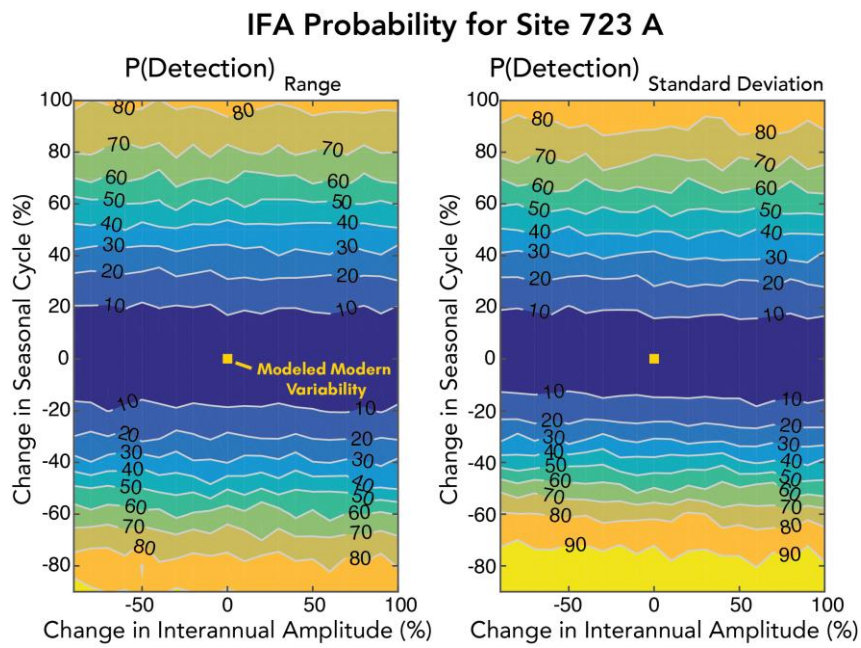


Figure 3. Individual foraminiferal analyses probability contour plot for range (left) and standard deviation (right) at Site 723 A, with modeled modern variability (yellow square), by definition at (0,0). Note that the probability contours are parallel to the Y-Axis (seasonality) and are insensitive to changes in interannual amplitude.

Formatted: Font: Bold, Complex Script Font: Bold

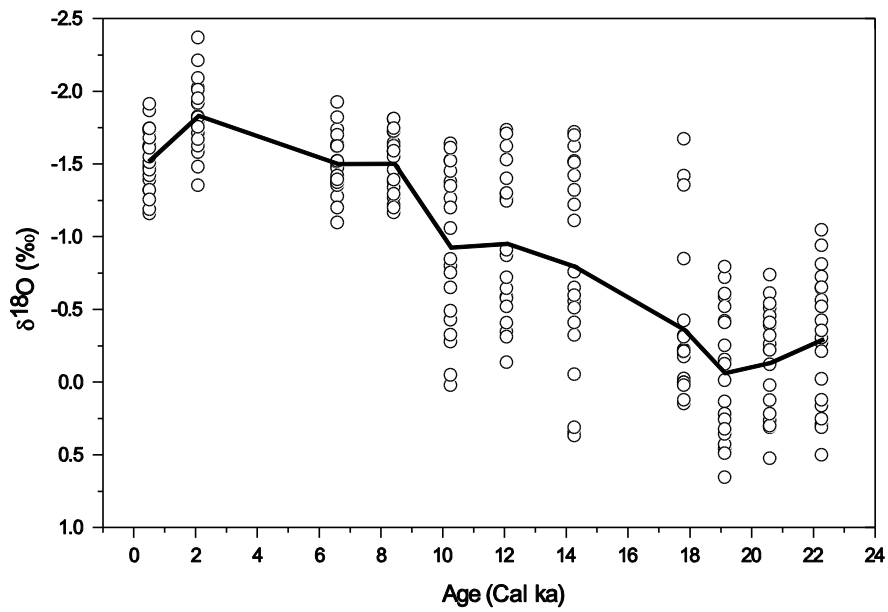


Figure 4. $\delta^{18}\text{O}$ values of individual *G. sacculifer* from the selected intervals, the line connects means value in each interval.

Formatted: Font: Bold, Complex Script Font: Bold

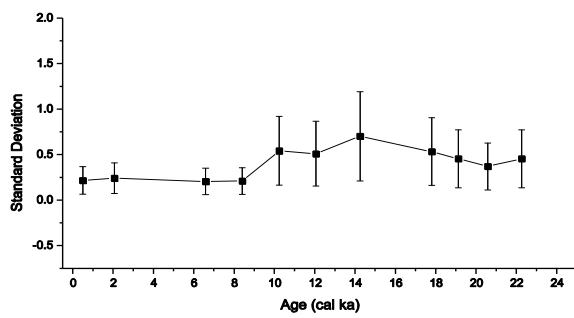


Figure 5. Standard deviation variations at specific time intervals, error bars of standard deviation are computed with 95% confidence levels.

Formatted: Font: Bold, Complex Script Font: Bold

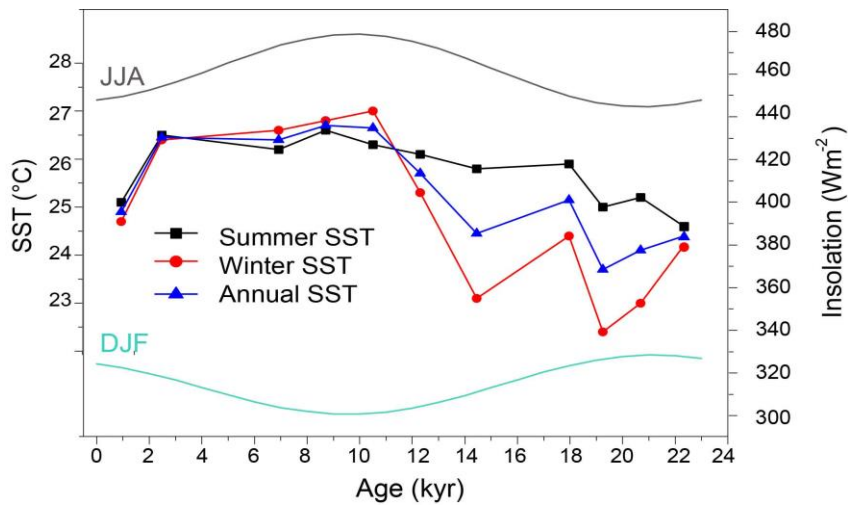


Figure 6. Fluctuations of summer, winter and annual SST derived from planktonic foraminifer abundances by using ANN technique at the ODP Site 723A (from Naidu and Malmgren, 2005). Solar insolation changes during June, July, August (JJA) and December, January, February (DJF) at 23°N latitude.

Formatted: Font: Bold, Complex Script Font: Bold

Table 1. AMS ¹⁴C dates used for establishing the chronology for ODP Site 723A
Naidu and Malmgren (2005).

S. No.	Depth (cm)	¹⁴ C Age	Calendar Years BP
1	3	950	280
2	16	1680	1005
3	39	2010	1330
4	64	2760	2254
5	96	3890	3587
6	121	4670	4622
7	154	6070	6276
8	186	7700	7938
9	218	8110	8359
10	274	9510	9854
11	316	10,500	10,877
12	520	15,920	18,200
13	740	19,130	22,260

Formatted Table

Table 2. Standard deviation values of *G. sacculifer* derived from individual shell analyses of $\delta^{18}\text{O}$ at the ODP site 723A. Significant standard deviations are shown in bold letters.

Age (ka)	<i>G. sacculifer</i> $\delta^{18}\text{O}$ Standard Deviation
0.50	0.22
2.07	0.24
6.59	0.21
8.41	0.21
10.24	0.54
12.06	0.51
14.25	0.7
17.81	0.53
19.12	0.45
20.58	0.37
22.26	0.45

Formatted Table

Table 3. Inter shell $\delta^{18}\text{O}$ variability of *G. sacculifer*, seasonal SST obtained from (Naidu and Malmgren, 2005), 0.25‰ $\delta^{18}\text{O}$ per 1°C and 0.22‰ $\delta^{18}\text{O}$ per 1 PSU were used.

Age (ka)	$\delta^{18}\text{O}$ inter shell std.dev. variability of <i>G. sacculifer</i> (‰)	Seasonal SST difference (°C)	$\delta^{18}\text{O}$ accounted by SST (‰)	$\delta^{18}\text{O}$ accounted by salinity (‰)	Seasonal salinity difference (PSU)
0.50	0.22	0.4	0.1	0.12	0.53
2.07	0.24	0.1	0.02	0.22	1.01
6.59	0.21	0.4	0.1	0.11	0.48
8.41	0.21	0.2	0.05	0.16	0.73
10.24	0.54	0.7	0.18	0.36	1.64
12.06	0.51	0.8	0.2	0.31	1.41
14.25	0.70	2.7	0.68	0.02	0.10
17.81	0.53	1.5	0.38	0.15	0.69
19.12	0.45	2.6	0.65	-0.20	-0.89
20.58	0.37	2.2	0.55	-0.18	-0.82
22.26	0.45	0.4	0.1	0.35	1.61